Research Article

Ecobiophysical Aspects on Nanosilver Biogenerated from *Citrus reticulata* Peels, as Potential Biopesticide for Controlling Pathogens and Wetland Plants in Aquatic Media

Marcela Elisabeta Barbinta-Patrascu,[1] **Nicoleta Badea,**[2]
Camelia Ungureanu,[2] **Stefan Marian Iordache,**[3] **Marioara Constantin,**[1]
Violeta Purcar,[4] **Ileana Rau,**[2] **and Cristian Pirvu**[2]

[1]*Faculty of Physics, Department of Electricity, Solid-State Physics and Biophysics, University of Bucharest, 405 Atomistilor Street, P.O. Box MG-11, 077125 Bucharest-Magurele, Romania*
[2]*Faculty of Applied Chemistry and Material Science, University "Politehnica" of Bucharest, 1-7 Polizu Str., 011061 Bucharest, Romania*
[3]*Faculty of Physics, 3 Nano-SAE Research Centre, University of Bucharest, P.O. Box MG-38, 077125 Bucharest-Magurele, Romania*
[4]*National Research & Development Institute for Chemistry and Petrochemistry-ICECHIM, 202 Splaiul Independentei, 6th District, P.O. Box 35-174, 060021 Bucharest, Romania*

Correspondence should be addressed to Nicoleta Badea; nicoleta.badea@gmail.com
and Camelia Ungureanu; ungureanucamelia@gmail.com

In recent years, a considerable interest was paid to ecological strategies in management of plant diseases and plant growth. Metallic nanoparticles (MNPs) gained considerable interest as alternative to pesticides due to their interesting properties. *Green* synthesis of MNPs using plant extracts is very advantageous taking into account the fact that plants are easily available and eco-friendly and possess many phytocompounds that help in bioreduction of metal ions. In this research work, we phytosynthesized AgNPs from aqueous extract of *Citrus reticulata* peels, with high antioxidant, antibacterial, and antifungal potential. These "green" AgNPs were characterized by modern biophysical methods (absorption and FTIR spectroscopy, AFM, and zeta potential measurements). The nanobioimpact of *Citrus*-based AgNPs on four invasive wetland plants, Cattail *(Typha latifolia)*, Flowering-rush *(Butomus umbellatus)*, Duckweed *(Lemna minor)*, and Water-pepper *(Polygonum hydropiper)*, was studied by absorption spectroscopy, by monitoring the spectral signature of chlorophyll. The invasive plants exhibited different behavior under AgNP stress. Deep insights were obtained from experiments conducted on biomimetic membranes marked with chlorophyll *a*. Our results pointed out the potential use of *Citrus*-based AgNPs as alternative in controlling pathogens in aqueous media and in management of aquatic weeds growth.

1. Introduction

Since its invention in 1959 [1], nanotechnology became the most fascinating area of science. Nowadays, the progress in nanotechnology opened new perspectives of metal nanoparticles (MNPs) applications in agriculture, in plant diseases or plant growth management [2, 3]. Among MNPs, silver nanoparticles (AgNPs) gained great popularity in various applications: biomedical, antimicrobial, antioxidant, antifungal, insecticidal, agriculture, and cosmetics industries [2, 4–11].

In last years, plant extracts were the most used resources in various fields: cosmetics [12], agriculture, and medicine [13], as environmentally benign inhibitor toward corrosion of carbon steel in acid media [14] or as precursor for biosynthesis of silver nanoparticles [8, 15–18].

The increasing interest in plants is due to their high abundance in nature, recyclability, and their content rich in bioactive principles. Contrary to chemical synthesis of AgNPs, which used toxic agents, the "green" synthesis of nanosilver using plant extracts is preferred today because it uses eco-friendly chemicals and raw materials.

Our work aimed to study the application of phytosynthesized AgNPs using an aqueous extract of *Citrus reticulata* (tangerine or mandarin) peels in management of water pond quality and control of invasive aquatic weeds.

In order to get deep insights about the action of AgNPs, the tests were firstly conducted *in vitro*, on mimicking photosynthetic membranes (artificial lipid bilayers loaded with chlorophyll *a*).

The studies were further performed on four common Romanian wetland plants: Cattail *(Typha latifolia)*, Flowering-rush *(Butomus umbellatus)*, Duckweed *(Lemna minor)*, and Water-pepper *(Polygonum hydropiper)*. They are invasive plants that rapidly reproduce and invade habitats, displacing many native species. Although these plants give a beautiful landscape and constitute a nutritional source for waterfowl or other birds and also provide protection for different aquatic creatures, they can become harmful in certain situations, when invading irrigation systems, fish lakes, or swimming pools, with dramatic consequences on *economy* (disrupting hydropower generation; impairment of commercial and recreational navigation; interfering with safe swimming and with fishing; endangering human health and increasing drowning risk; impairing drinking water, etc.) and *ecology* (suppression of desirable native plants; reducing species diversity; water quality degradation; alteration of animal community interactions; fish killing, etc.) [20]. Uncontrolled growth of these invasive species can be stopped with pesticides, but these chemicals could be harmful for human health and the environment, too. So, novel methods, safer and environmental benign, must be imposed to overcome these problems. Thus, AgNPs biogenerated from *C. reticulata* peels extract (*Citrus*-nAg) were tested for application in controlling phytopathogens and invasive plants in aquatic media. *Citrus*-nAg were firstly characterized by spectral methods (absorption and FTIR spectroscopy), and morphological aspects were obtained from AFM investigations. The stability of *Citrus*-nAg was checked by zeta potential measurements. Further investigations on bioactivities of *Citrus*-nAg demonstrated their antioxidant, antibacterial, and antifungal properties. The bioimpact on the tested wetland plants was assayed by treating these herbs with increasing concentrations of *Citrus*-nAg and monitoring the spectral signature of chlorophyll (Chl).

2. Materials and Methods

2.1. Materials. Soybean lecithin (Calbiochem), KH_2PO_4, Na_2HPO_4, peptone, HCl, H_2O_2, luminol (5-amino-2,3-dihydrophthalazine-1,4-dione), and Tris (hydroxymethyl aminomethane base) were purchased from Merck (Germany). Silver nitrate ($AgNO_3$) was supplied by Gatt Koller-GmbH, Austria. NaCl, 69% HNO_3, and 37% HCl were

purchased from Sigma-Aldrich (Germany). The yeast extract was obtained from Biolife and the agar from Fluka.

Chlorophyll a (Chl*a*) was obtained in our laboratory from fresh spinach (*Spinacia oleracea* L.) leaves by a chromatographic method as previously described [21, 22], and the purity of this phytopigment was checked by Vis absorption spectra.

2.2. Sample Preparation

2.2.1. Preparation of Citrus reticulata Peels' Extract. Fresh tangerine peels thoroughly washed with distilled water and dried with filter paper were cut into small pieces and then mixed with distilled water in a final mass ratio *Citrus* peels/distilled water of 1:3 (w/w). The as-prepared mixture was boiled for 5 minutes. After cooling at room temperature and in dark, it was filtered with Whatman filter paper number 1 and then kept in freezer.

2.2.2. Biosynthesis of AgNPs from Citrus reticulata Peels' Extract (Citrus-nAg). An amount of 34 mg $AgNO_3$ was added to 50 mL aqueous extract under continuously stirring at room temperature. The biosynthesis of nanosilver from *C. reticulata* peels' extract (named *Citrus*-nAg) was visually observed via color change of this mixture. Tangerine peel extract, which is eco-friendly, acted as both a reducing and a stabilizing agent.

2.2.3. Preparation of Biomimetic Membranes Marked with Chla. Small unilamellar vesicles (SUVs) labeled with Chl*a* were prepared according to [23, 24], by hydrating a soybean lecithin/Chl*a* (100:1, molar ratio) thin film with phosphate buffer (PB, KH_2PO_4-Na_2HPO_4 pH 7.4), followed by mechanical stirring (VIBRAX stirrer-OHIO 43230, USA, 200 rpm, 40 min), and then subjected to ultrasound treatment (Hielscher Ti probe sonicator, UP 100 H-Hielscher Ultrasonics GmbH, 14513 Teltow, Germany).

2.3. Characterization Methods. The *absorption spectra* were recorded in the 200–800 nm wavelength range on a double beam Lambda 2S Perkin Elmer UV-Vis spectrophotometer, operated at a resolution of 1 nm.

The fluorescence emission spectra of Chl*a* in biomimetic membranes were collected in the wavelength range of 600–800 nm, on a LS55 Perkin Elmer fluorescence spectrometer, by illuminating the samples with 430 nm excitation wavelength.

FTIR spectra of samples were obtained using a Fourier Transform Infrared Spectrophotometer (Tensor 37 from Bruker). For all of the scans, the spectra were collected in the wavenumber range of 400–4000 cm^{-1}, at a spectral resolution of 4 cm^{-1}.

The silver content in the AgNP suspension was determined by atomic absorption spectroscopy, AAS (ContrAA 700, Analytik Jena, Germany), after microwave assisted acid digestion (Milestone, SUA). In order to quantify the silver ion concentration released in time, the AgNP stock suspension was subjected to centrifugation (21000 ×g for 30 minutes, at 0°C, SIGMA 2–16K centrifuge) at different periods. All

measurements were performed in triplicate. Prior to AAS analysis, approximately 0.5 g of each sample was completely digested using a mixture of 69% HNO_3, 37% HCl, and 30% H_2O_2.

The morphology of silver nanoparticles was analyzed using an APE Research A100-SGS (Italy) atomic force microscope (AFM), working in contact mode system. Gwyddion software was used to process AFM images.

Zeta potential (ZP) measurement was carried out in an appropriate device of Zetasizer Nano ZS (Malvern Instruments Ltd., UK), by applying an electric field across the analyzed aqueous suspension.

The in vitro antioxidant activity (AA%) of *Citrus*-nAg was assayed through chemiluminescence method on a Chemiluminometer Turner Design TD 20/20 (USA), by using the system containing: luminol (1 mM), Tris-HCl buffer solution (pH 8.6), and H_2O_2 (10 μM), as free radical generator. The value of AA% was expressed as

$$\text{AA} = \left[\frac{(I_0 - I)}{I_0} \right] \cdot 100\%, \tag{1}$$

where I_0 is the maximum CL intensity at $t = 5$ s, for the reaction mixture without the sample, and I is the maximum CL intensity for each sample, at $t = 5$ s [25].

For determination of *Minimum Inhibitory Concentration* (MIC value recorded is defined as the lowest concentration of the assayed antimicrobial agent that inhibits the visible growth of the microorganism tested, and it is usually expressed in μg/mL) of *Citrus*-nAg against the tested microbial strains, each of the tested microorganisms was determined by the broth dilution technique [26]. Serially diluted logarithmic concentrations of the *Citrus*-nAg ranging from 400 μg/mL to 0.195 μg/mL were inoculated with standardized overnight cultures of the microorganisms and incubated at 37°C. Dilution methods are the most appropriate ones for the determination of MIC values, since they offer the possibility of estimating the concentration of the tested antimicrobial agent in the broth medium [27]. The most recognized standards are provided by the CLSI and the European Committee on Antimicrobial Susceptibility Testing (EUCAST) [28]. The MIC assay was performed in triplicate.

In order to evaluate the *antibacterial activity*, the *Citrus*-nAg were tested against pathogenic *Escherichia coli* ATCC 8738 microbial strain. The bacterial strains were grown in Luria Bertani Agar (LBA) plates at 37°C with following composition: peptone (10 g/L); yeast extract (5 g/L), NaCl (5 g/L); and agar (20 g/L). The stock culture was maintained at 4°C.

Antifungal activity of *Citrus*-nAg was tested against the fungal aquatic pathogen *Fusarium oxysporum* ATCC 48112. The stock culture was maintained at 4°C. These strains were cultivated onto potato-dextrose agar (abbreviated "PDA") from Sigma-Aldrich Company with next composition: potato extract (4 g/L), dextrose (20 g/L), and agar (15 g/L).

Time-kill test is the most appropriate method for determining the bactericidal or fungicidal effect. The time-kill test reveals a time-dependent or a concentration-dependent antimicrobial effect [28, 29]. For bacteria, this test has been well standardized and described in M26-A document of CLSI [30]. Similarly, several antifungal substances were studied by this method [31, 32].

Time-kill test for determining the bactericidal effect was performed in broth culture medium using three tubes containing a bacterial suspension of $5 \cdot 10^5$ CFU/mL (colony-forming units/mL). The first and the second tubes contain the extract tested usually at final concentrations of 0.25 MIC and 1 MIC, and the third one is considered as the growth control. 1 mL of each tube was placed onto Bacto-Agar plates. The incubation was done under suitable conditions for 24 h at 37°C to determine the number of viable *E. coli* in terms of CFU. Then, the percentage of dead cells was calculated relatively to the growth control by determining the number of living cells (CFU/mL) of each tube using the agar plate count method [33].

Time-Kill Test for Determining the Fungicidal Effect. The agar dilution method involves the incorporation of varying desired concentrations (1 MIC and 0.25 MIC) of the Citrus-nAg into an agar medium, followed by the inoculation of a *Fusarium oxysporum* inoculum onto the agar plate surface. The plates were incubated for 4-5 days at 37°C to see the fungicidal effect [34].

Standard deviation was calculated as the square root of variance using STDEV function in *Excel* 2010.

3. Results and Discussion

3.1. Characterization of Silver Nanoparticles Biosynthesized from Tangerine Peel Extract. The biosynthesis of silver nanoparticles from aqueous extract of *C. reticulata* peels was firstly monitored by visual inspection. Thus, after addition of silver ions, the color of tangerine extract turned from orange to dark brown (Figure 1).

The green synthesis of AgNPs was further confirmed by spectral characterization (Figure 2) and AFM analysis (Figure 3). The absorption spectra (Figure 2(a)) showed that, after adding silver nitrate to vegetal extract, a SPR band appeared at 443 nm, which is characteristic for spherical/quasi-spherical silver nanoparticles [8, 35].

The FTIR transmission spectrum (Figure 2(b)) of aqueous *C. reticulata* extract showed presence of IR bands at 3850, 3740, and 3321 cm^{-1} (characteristic of O–H stretching of hydroxyls), 2355 and 2112 cm^{-1} (N–H stretching vibrations), 1740 cm^{-1} (C=O cm^{-1} stretching attributed to aldehyde, ketones, carboxylic acid, or pectin ester), 1639 cm^{-1} (attributed to amide I; pectin), 1368 cm^{-1} (C–CH3 bending), 1218 cm^{-1} (C–O stretch acidic or ν_{as}(C–O–C) of geranyl acetate (acyclic monoterpene)), 1110 cm^{-1} (ν(CO), ν(CC) ring of polysaccharides, and pectin), 1082 cm^{-1} and 1068 cm^{-1} (may be due to alcohol, carboxylic acid and esters), and 641 cm^{-1} (assigned to bending modes of aromatic compounds) [11, 15, 36–38].

After bioreduction of silver ions, the following events were observed:

(1) The FTIR bands at 3850, 3740, 1740, and 1639 cm^{-1} were shifted to 3857, 3743, 1747, and 1633 cm^{-1},
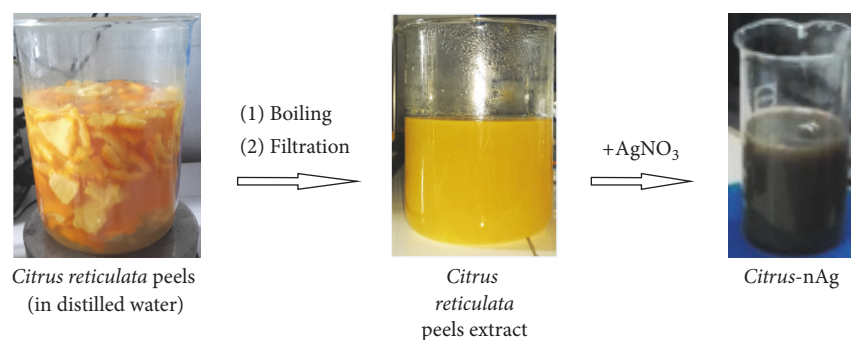
FIGURE 1: Schematic representation of AgNPs biosynthesis from *Citrus reticulata* peels extract.

respectively, becoming strong and sharps (3857 and 3743 cm^{-1}) and weaker (1747 and 1633 cm^{-1}).

(2) The peaks at 3857 and 3743 are more strong and sharp, while that at 1633 cm^{-1} weakened.

(3) The band at 1068 cm^{-1} shifted to 1060 cm^{-1} and became stronger in AgNP spectrum.

(4) New peak was observed in the FTIR spectrum of *Citrus*-nAg: 2927 cm^{-1} (alkyls C–H stretching) [39].

On the other hand, both *Citrus* extract and AgNPs presented broad strong FTIR peaks at 3321 and 3384 cm^{-1}, respectively, suggesting the presence of stretch hydrogen bonding. It could be observed from the FTIR spectra of *Citrus reticulata* peels extract and of *Citrus*-nAg that hydroxyl and carboxyl groups are predominant.

Our IR results confirmed that phytomolecules like pectin, polyphenols, and proteins played an important role in the bioreduction of silver ions, these biomolecules acting as both reducing and capping agents for silver nanoparticles.

The physical stability of AgNPs was evaluated in terms of zeta potential measurements, via their electrophoretic mobility in an electric field [40]. The obtained ZP value showed that the "green" synthesized AgNPs are quite stable (ZP = −21.9 mV), their physical stability being achieved through interparticle repulsion forces, due to the presence onto their surface, of the carboxyl groups arising from *Citrus reticulata* peels extract (see Figure 2(b)).

Few drops of *Citrus*-nAg suspension were deposited on a silica glass plate and allowed to dry at room temperature in the dark, and then the resulting thin film was analyzed by AFM. Figure 3 illustrates the morphological aspects in three-dimensional AFM image (a) and line profile (b) of *Citrus*-nAg. As observed, spherical silver nanoparticles with nanoscaled dimension (mean diameter < 135 nm) and good dispersion were obtained by a green route from tangerine peels. The shape of AgNPs was firstly predicted by absorption spectrum and then confirmed by AFM analysis. The average roughness (the arithmetic average texture of one surface) provided by AFM images was R_a = 28.4 nm, and the root mean square parameter (R_{ms}) reached the value of 36.6 nm.

The AAS results indicated that the concentration of AgNP stock suspension was 538.3 ppm. The high toxicity of silver ions is well known [41], that is why the silver content was

determined in the supernatants (which contain silver ions) of the *Citrus*-nAg suspensions taken at different times after *Citrus*-nAg preparation.

The supernatants collected one hour and five hours after addition of silver nitrate to tangerine extract contained silver in concentration of 191.1 and 92.4 ppm, respectively, indicating that the silver bioreduction was not finished after 5 h, and Ag$^+$ was still present in suspension. On the contrary, the silver content was 0 ppm in the supernatants collected after 1, 2, 3, and 7 days, indicating that Ag$^+$ was not present in any supernatant, the *Citrus*-nAg being stable even after 7 days.

3.2. The Bioactivities of Citrus-nAg.

The *in vitro antioxidant activity assay* revealed high potential of *Citrus*-nAg of free radical scavenging, through chemiluminescence method. Their antioxidant activity reached the value of 98.5%. Two main factors are responsible for this strong antioxidant potential:

(1) the presence of antioxidant biomolecules (like polyphenols, pectin, etc.) coming from tangerine peel extract (see Figure 2(b)) as capping agents of AgNPs [42];

(2) the nanodimensions of *Citrus*-nAg (Figure 3), which offer high total surface area providing many reaction centres that improve the free radical scavenging capacity [8, 43].

As known, usual microbial contaminants of aquatic media are *Escherichia coli* and *Fusarium oxysporum*, which can cause severe diseases [44–48], especially to the immuno-compromised hosts [49] so the antimicrobial investigations were conducted on *E.coli* ATCC 8738 bacterium and *Fusarium oxysporum* ATCC 48112 fungus.

Results obtained for the antimicrobial susceptibility test of *Citrus*-nAg on the organism showed MIC of 25 ± 0.19 and 12.5 ± 0.13 μg/mL against *Escherichia coli* and *Fusarium oxysporum*, respectively (see Table 1).

Antimicrobial susceptibility was determined on 3 different days, and MIC values for each isolate were reported as the median of 3 experiments.

The *C. reticulate*-based AgNPs exhibited strong *antibacterial activity* against *E.coli* ATCC 8738 (Figure 4). On the plate corresponding to the *Citrus*-nAg, 1 MIC (25 μg/mL), *E. coli*
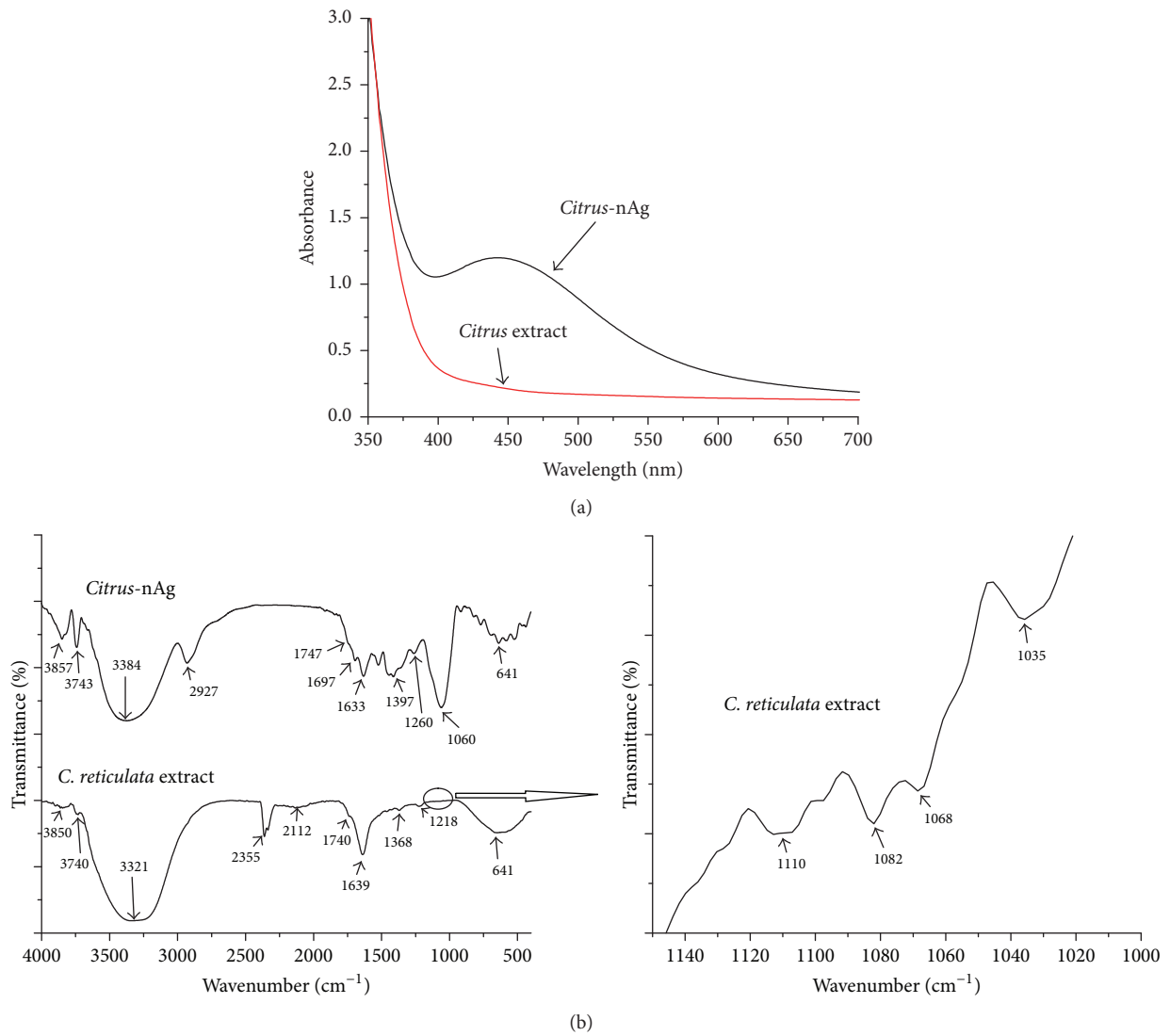
(a)

(b)

Figure 2: Comparative spectral characterization of aqueous *C. reticulata* extract and *Citrus*-nAg by (a) absorption and (b) FTIR spectroscopy.
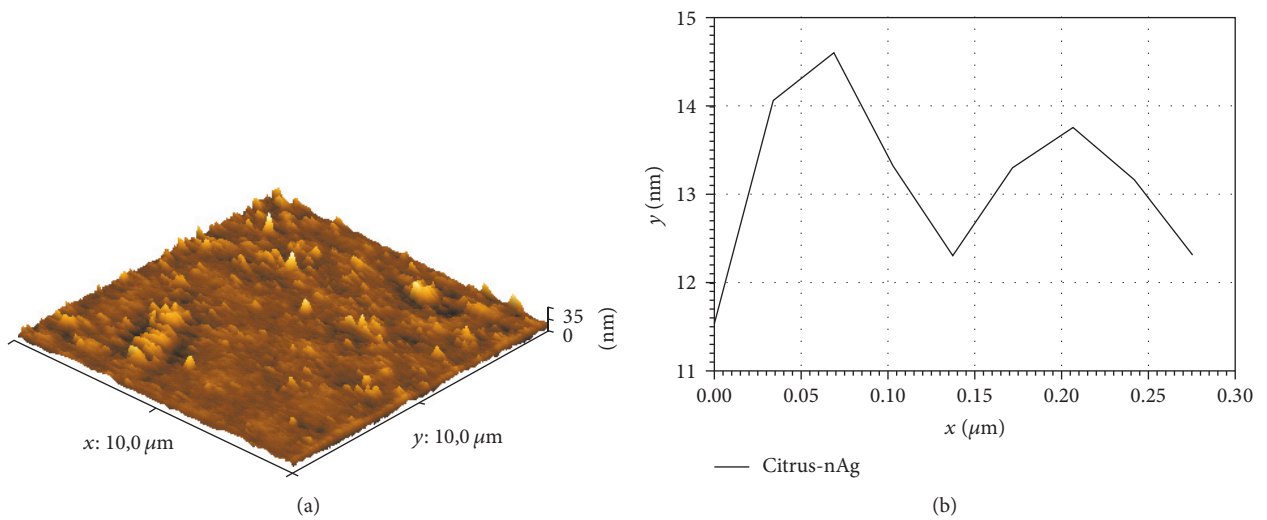

(a)

(b)

Figure 3: Three-dimensional AFM image (a) and line profile (b) of *Citrus*-nAg.

TABLE 1: Antimicrobial susceptibility of the microorganisms to *Citrus*-nAg.

Microorganism	Concentration of *Citrus*-nAg used (μg/mL)											
	400	200	100	50	25	12.5	6.25	3.125	1.56	0.78	0.39	0.195
Escherichia coli	S	S	S	S	S	R	R	R	R	R	R	R
Fusarium oxysporum	S	S	S	S	S	S	R	R	R	R	R	R

Note. R: resistant; S: susceptible/sensitive.

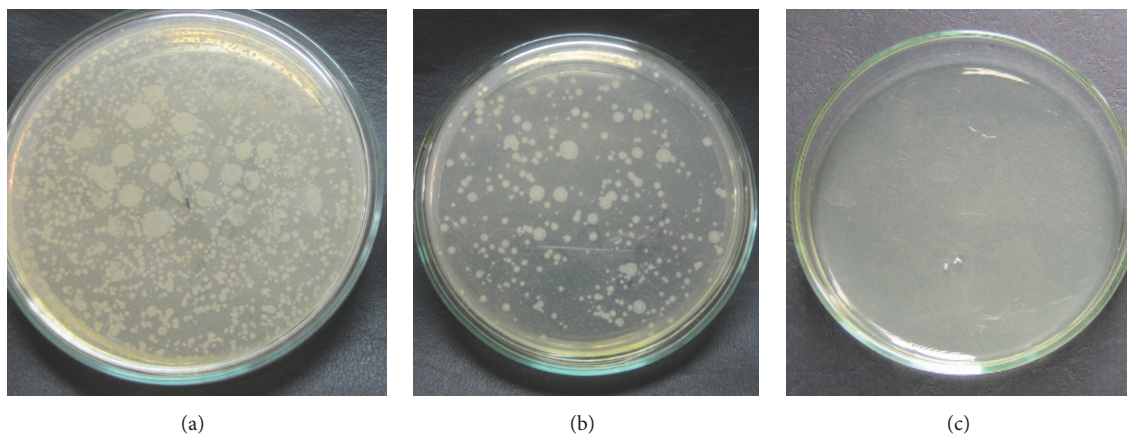(a)   (b)   (c)

FIGURE 4: Bacto-Agar plates with CFU of *E. coli* to determine the Time-kill (concentration-dependent antimicrobial effect) of (a) growth control, (b) *Citrus*-nAg, 0.25 MIC, and (c) *Citrus*-nAg, 1 MIC.

culture was inhibited (0 CFU/mL of *E. coli*), confirming the antibacterial effect of this sample (Figure 4(c)). In the plates corresponding to the *Citrus*-nAg, 0.25 MIC (6.25 μg/mL), a more pronounced growth of *E. coli* was noticed ($248 \cdot 10^3 \pm 0.22$ CFU/mL).

This microbial response is due to the presence on the AgNP surface of the capping biomolecules arising from *C. reticulata* peels (see Figure 2(b)), which have antibacterial properties (pectin, flavonoids, etc.). As observed, *Citrus*-nAg has great potential for application as disinfectant for pools, ponds, or different aquatic basins.

The antifungal activity investigation of the biogenerated AgNPs was performed as previously described (see Section 2.3). Fungicidal activity of *Citrus*-nAg against *Fusarium oxysporum* ATCC 48112, a commonly occurring fungal aquatic pathogen, is illustrated in Figure 5.

Citrus-AgNPs showed a significant effect on morphological structure of this fungus (Figure 6(b)); it induced important changes in the macroscopic appearance of fungal colonies (near halo) and the colonies appeared white and adherent to the surface of the medium. In most cases, the addition of *Citrus*-nAg led to smaller colonies and partial loss of spore formation (see as colorless colonies).

Light microscopic observation on *Fusarium oxysporum* hyphae exposed to AgNPs revealed considerable morphological alterations in hyphae; these appeared degraded and large vesicles are also visible.

Light microscopy of untreated fungi revealed normal mycelia; however hyphae of the strains grown on media with *Citrus*-nAg revealed alterations in the morphology of the hyphae and in the sporulation process.

The antifungal activity of these silver nanoparticles is maybe due to their capacity of anchoring to the surface of fungal cells destructing the membrane integrity [50], which caused the cell death. Another key factor responsible for this antifungal ability of *Citrus*-nAg is the presence of phytomolecules (flavonoids, pectin, volatile oils, etc.), arising from *Citrus reticulata* peels extract, as capping agents for *Citrus*-nAg, with fungicide properties [51–53].

3.2.1. The Impact of Citrus-nAg on Biomimetic Membranes. In order to get more information (at molecular level) about the action of *Citrus*-nAg on the wetland plants, we firstly studied the influence of these nanosilver particles on mimicking cell membranes, because the biomembranes are the first target for any stressor. Increasing concentrations of *Citrus*-nAg were added to a suspension of biomimetic membranes marked with Chl*a*, which were characterized by absorption and emission spectroscopy (Figure 7). Chl*a* acted as a spectral marker that detects the changes occurring in artificial lipid bilayers. It was observed that the height of the red absorption peak (Figure 7(a)) was reduced under AgNP stress.

Chl*a* fluorescence quenching occurred in *Citrus*-nAg-stressed biomimetic membranes (Figure 7(b)), action that is possible due to an electron-transfer or an energy-transfer process when the fluorophore, which is the porphyrin ring of chlorophyll, attached directly to the surface of AgNPs [54, 55].

3.2.2. The Bioimpact of Citrus-nAg on Wetland Plants. The effects of *Citrus*-nAg on four native wetland plants, *Typha latifolia*, *Butomus umbellatus*, *Lemna minor*, and *Polygonum*
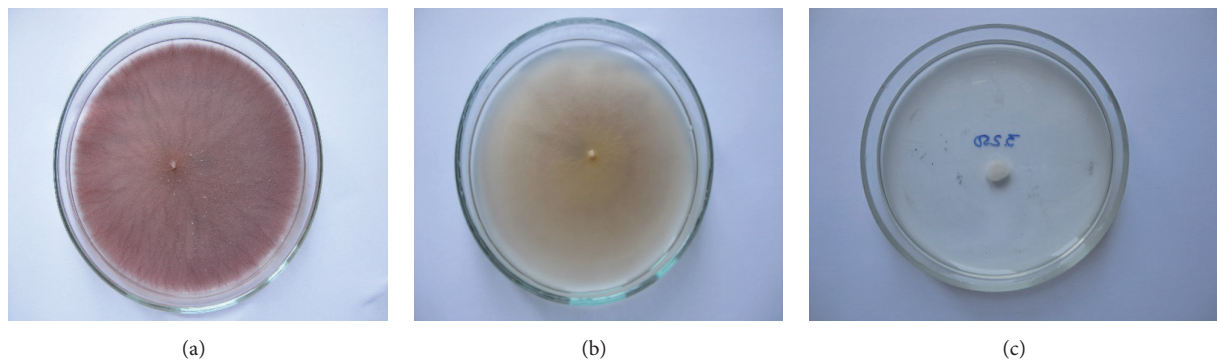
(a) (b) (c)

FIGURE 5: Agar plates with *Fusarium oxysporum* to determine the Time-kill (concentration-dependent antimicrobial effect) of (a) growth control, (b) *Citrus*-nAg, 0.25 MIC, and (c) *Citrus*-nAg, 1 MIC.
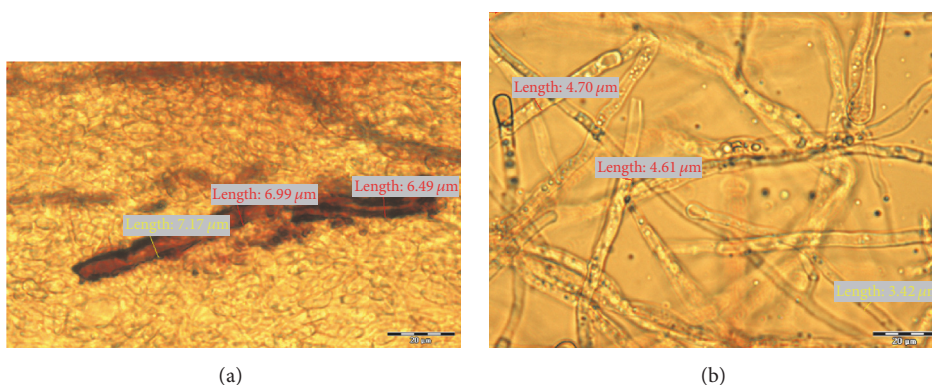

(a) (b)

FIGURE 6: The microscopic aspect of reproductive formations for *Fusarium oxysporum*: (a) before and (b) after treatment with *Citrus*-nAg (scale of 20 μm).
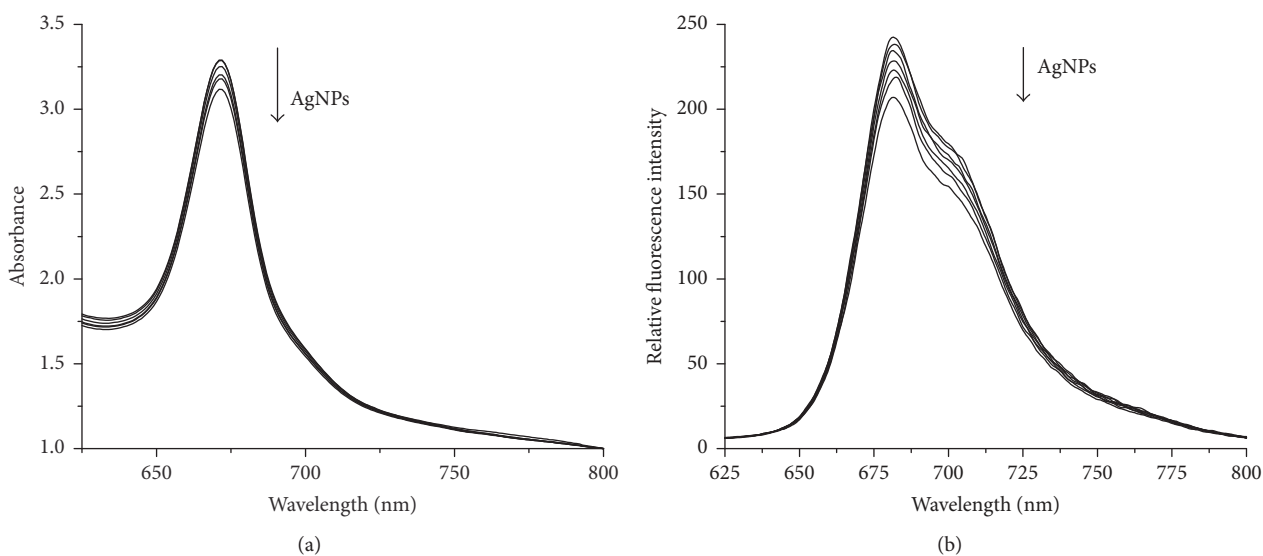

(a) (b)

FIGURE 7: Spectral monitoring of AgNP effects on biomimetic membranes marked with Chl*a*: the absorption (a) and the fluorescence emission (b) spectra. The absorption spectra were corrected for the contribution of light scattering as described in [19] and normalized at 800 nm. In the fluorescence experiments, the excitation wavelength was 430 nm.

Rush, cattail
(Typha latifolia)

Flowering-rush
(Butomus umbellatus)

Duckweed
(Lemna minor)

Water-pepper
(Polygonum hydropiper)

FIGURE 8: The images of the four native wetland plants: *Typha latifolia, Butomus umbellatus*, *Lemna minor*, and *Polygonum hydropiper* studied in this work.

hydropiper (Figure 8), were studied. These plants were collected from a natural lake in a park from Oltenita, a Romanian city.

The plants (about two months aged) were treated with increasing concentrations of *Citrus*-nAg (0.42, 0.84, 1.675, 3.35, 6.7, 13.4, 26.8, and 53.5 ppm) and then visually monitored for two weeks. No significant alterations of herbals were observed with the naked eye at *Citrus*-nAg concentrations less than 13.4 ppm. In all cases, the concentration of 13.4 ppm was critical, because at this concentration of AgNPs, visible modifications on plant morphology could be observed. At concentrations greater than 13.4 ppm, the plants were died. Flowering-rush and Water-pepper were the most sensitive: they started withering after four days of AgNPs-stress. On the contrary, the rush withered just after two weeks. Duckweed was the most resistant; in this case, visible modifications were observed only at AgNP concentration greater than 13.4 ppm.

These visual observations were further confirmed by spectral characterization of the vegetal extracts prepared by shredding the leaves of each wetland plants, in distilled water

(the mass ratio leaves/water was 1 : 10). In this respect, we compared the absorption spectra of the extracts prepared from AgNPs (13.4 ppm)-stressed plants with that of untreated ones (Figure 9).

Chlorophyll (Chl) was chosen as an indicator of plant quality. Chl is a key molecule in photosynthesis and plays a vital role for higher plants surviving. The level of Chl is an indicator of physiological status of plants, any change of Chl absorption or Chl fluorescence reflecting the level of photosynthesis [56].

Monitoring the absorption band at the main red peak of Chls, which is a spectral signature of these porphyrins, a decline of this band was observed and hence a decrease in chlorophyll content after nAg stress. This process was also observed in the previous assay performed on biomimetic membranes (see Figure 7). The intensity of the main red peak characteristic for Chl decreased under nAg stress, but in the case of *Butomus umbellatus*, this band disappeared.

Similar behavior was found by Miao and coworkers [57], which observed a reduction of plant growth, photosynthesis,
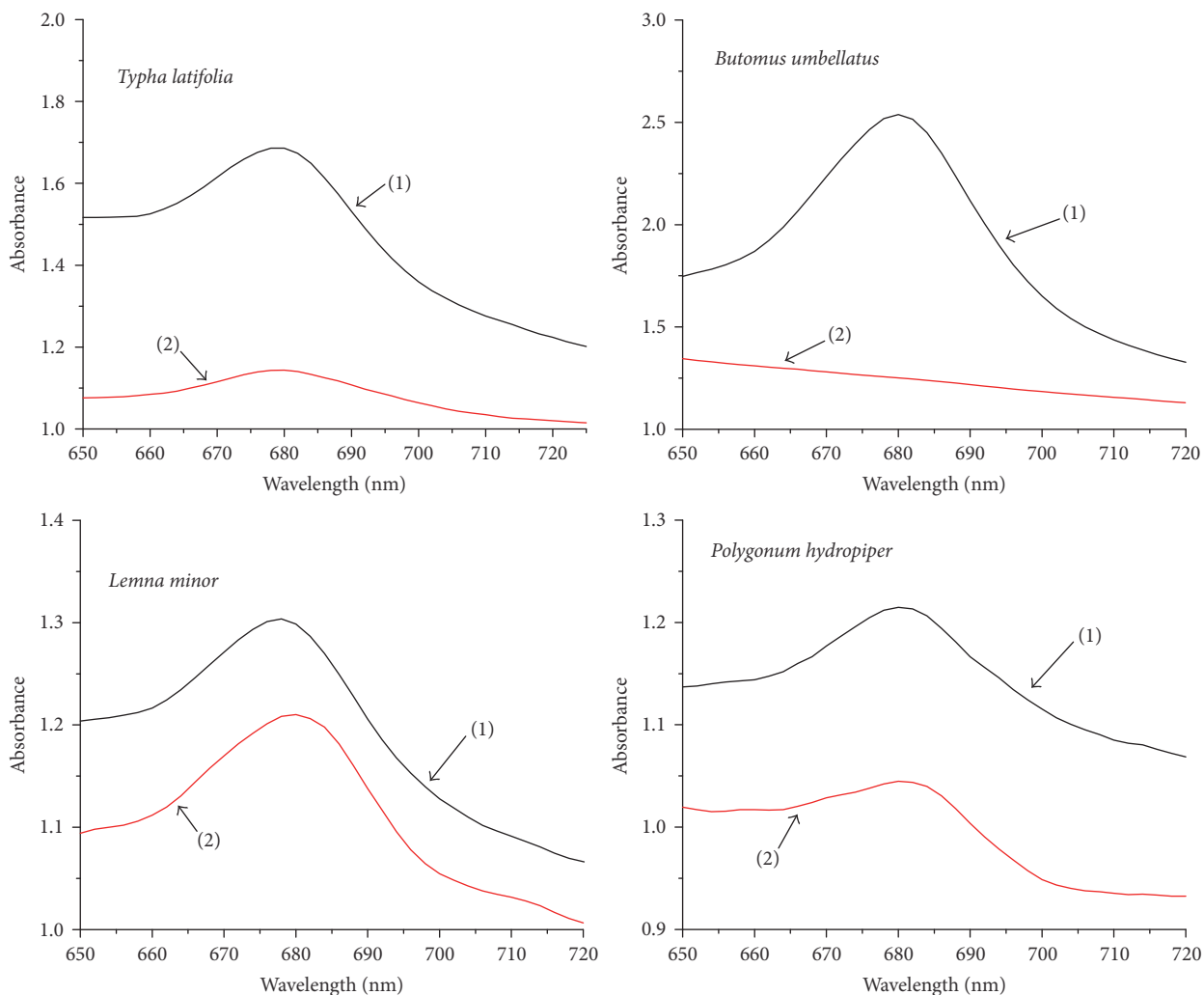
FIGURE 9: The absorption spectra of the wetland plant extracts: before (1) and after (2) treatment with *Citrus*-nAg (13.4 ppm).

and chlorophyll production in algae after AgNP treatment. Barbasz et al. highlighted that MNPs significantly affected the physiological properties of plants [58].

In our work, the bioimpact of *Citrus*-nAg on wetland plants was more pronounced in the case of *Butomus umbellatus* and nonsignificant in the case of *Lemna minor*. These findings are in accordance with our visual observations and with the experiments on artificial cell membranes (Figure 7).

Based on these results, we can concluded that *Citrus*-nAg enter into cell membranes and could induce physiological changes in plants (in a dose-dependent manner), by altering also the chlorophyll content.

4. Conclusions

An eco-friendly method was employed to biogenerate nanosilver, by using the aqueous extract of *Citrus reticulata* peels that proved to be very good bioreductant of silver ions for the synthesis of AgNPs. The biosynthesized AgNPs exhibited strong antimicrobial activity against *Fusarium oxysporum* ATCC 48112 fungus and *Escherichia coli* ATCC 8738 bacterium and also high antioxidant capacity.

The bioeffect of *Citrus*-nAg on four living wetland plants (*Typha latifolia*, *Butomus umbellatus*, *Lemna minor*, and *Polygonum hydropiper*) was studied through both *in vivo* and *in vitro* assays, by choosing the natural photopigment, *chlorophyll*, as an indicator of plant quality. A dose-dependent effect of AgNPs on the tested plants was observed. Furthermore, the optical signature of chlorophyll embedded in biomimetic membranes offered useful information about *Citrus*-nAg stress, at molecular level. The exposure to *Citrus*-nAg at an appropriate concentration could only sanitize the aquatic basins, keeping intact the weed flora. But in certain concentrations, these AgNPs could kill even the invasive plants.

The use of phytosynthesized AgNPs in aquatic media is a safer procedure, because the capping agents are biogenic and benign for environment.

Our results suggest that this "green" nanosilver biogenerated from aqueous extract of *Citrus reticulata* peels could be used in fabrication of eco-friendly disinfectants to fight against fungi and bacteria in wet media (swimming pools, shower drainages, SPA retreats, water filters, wetlands, etc.) and also in herbicidal nanoformulations to manage and keep under control the invasive aquatic plants.

Conflicts of Interest

The authors declare that there are no conflicts of interest regarding the publication of this paper.
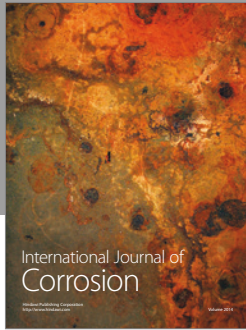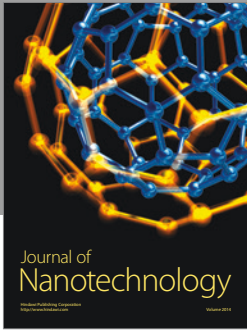
Acknowledgments

References

[1] M. K. Sarmast and H. Salehi, "Silver Nanoparticles: An Influential Element in Plant Nanobiotechnology," *Molecular Biotechnology*, pp. 1–9, 2016.

[2] A. D. Servin and J. C. White, "Nanotechnology in agriculture: Next steps for understanding engineered nanoparticle exposure and risk," *NanoImpact*, vol. 1, pp. 9–12, 2016.

[3] M. R. Khan and T. F. Rizvi, "Nanotechnology: Scope and Application in Plant Disease Management," *Plant Pathology Journal*, vol. 13, no. 3, pp. 214–231, 2014.

[4] P. A. De León-Martínez, F. Soriano-Corral, C. A. Ávila-Orta et al., "Surface Modification of nTiO$_2$/Ag Hybrid Nanoparticles Using Microwave-Assisted Polymerization in the Presence of Bis(2-hydroxyethyl) Terephthalate," *Journal of Nanomaterials*, vol. 2017, Article ID 7079497, pp. 1–9, 2017.

[5] J. Pulit-Prociak and M. Banach, "Silver nanoparticles—a material of the future...?" *Open Chemistry*, vol. 14, no. 1, pp. 76–91, 2016.

[6] G. A. M. Abdelmalek and T. A. Salaheldin, "Silver Nanoparticles as a Potent Fungicide for Citrus Phytopathogenic Fungi," *Journal of Nanomedicine Research*, vol. 3, no. 5, 8 pages, 2016.

[7] M. E. Barbinta-Patrascu, N. Badea, C. Pirvu et al., "Multifunctional soft hybrid bio-platforms based on nano-silver and natural compounds," *Materials Science and Engineering C*, vol. 69, pp. 922–932, 2016.

[8] M. E. Barbinta-Patrascu, N. Badea, C. Ungureanu, M. Constantin, C. Pirvu, and I. Rau, "Silver-based biohybrids "green" synthesized from Chelidonium majus L.," *Optical Materials*, vol. 56, pp. 94–99, 2016.

[9] M. A. Franco-Molina, E. Mendoza-Gamboa, D. G. Zarate-Triviño et al., "In Vitro evaluation of colloidal silver on immune function: antilymphoproliferative activity," *Journal of Nanomaterials*, vol. 2016, 8 pages, 2016.

[10] S. Mishra and H. B. Singh, "Biosynthesized silver nanoparticles as a nanoweapon against phytopathogens: exploring their scope and potential in agriculture," *Applied Microbiology and Biotechnology*, vol. 99, no. 3, pp. 1097–1107, 2014.

[11] H. P. Borase, C. D. Patil, R. B. Salunkhe, C. P. Narkhede, B. K. Salunke, and S. V. Patil, "Phyto-Synthesized Silver Nanoparticles: A Potent Mosquito Biolarvicidal Agent," *Journal of Nanomedicine Biotherapeutic Discovery*, vol. 3, no. 1, pp. 10–4172, 2013.

[12] A. Ribeiro, M. Estanqueiro, M. Oliveira, and J. Sousa Lobo, "Main Benefits and Applicability of Plant Extracts in Skin Care Products," *Cosmetics*, vol. 2, no. 2, pp. 48–65, 2015.

[13] A. Giordano and A. Costs, Eds., *Plant extracts: role in agriculture, health effects and medical applications (botanical research and practices)*, vol. 14, Nova Science Pub Inc, 1st edition, 2013.

[14] A. Cojocaru, I. Maior, D.-I. Vaireanu, I. Lingvay, C. Lingvay, and S. Caprarescu, "Estimation of inhibition efficiency for carbon steel corrosion in acid media by using natural plant extracts," *Revista de Chimie*, vol. 60, no. 11, pp. 1175–1180, 2009.

[15] M. E. Barbinta-Patrascu, I.-R. Bunghez, S. M. Iordache, N. Badea, R.-C. Fierascu, and R. M. Ion, "Antioxidant properties of biohybrids based on liposomes and sage silver nanoparticles," *Journal of Nanoscience and Nanotechnology*, vol. 13, no. 3, pp. 2051–2060, 2013.

[16] M. E. Barbinta-Patrascu, C. Ungureanu, S. M. Iordache et al., "Eco-designed biohybrids based on liposomes, mint-nanosilver and carbon nanotubes for antioxidant and antimicrobial coating," *Materials Science and Engineering C*, vol. 39, no. 1, pp. 177–185, 2014.

[17] S. Roy and T. K. Das, "Plant mediated green synthesis of silver nanoparticles-a review," *International Journal of Plant Biology and Research*, vol. 3, no. 3, pp. 1044–1055, 2015.

[18] F. E. Meva, C. O. Ebongue, S. V. Fannang et al., "Natural Substances for the Synthesis of Silver Nanoparticles against Escherichia coli: The Case of Megaphrynium macrostachyum (Marantaceae), Corchorus olitorus (Tiliaceae), Ricinodendron heudelotii (Euphorbiaceae), Gnetum bucholzianum (Gnetaceae), and Ipomoea batatas (Convolvulaceae)," *Journal of Nanomaterials*, vol. 2017, Article ID 6834726, 6 pages, 2017.

[19] M. B. Patrascu, L. Tugulea, A. Meghea, and A. Popescu, "Oxidative stress on liposomes with chlorophyll*a* monitored by spectral studies," *Optoelectronics and Advanced Materials – Rapid Communications*, vol. 2, no. 2, pp. 113–116, 2008.

[20] L. A. Gettys, W. T. Haller, and D. G. Petty, Eds., *Biology and Control of Aquatic Plants: A Best Management Practices Handbook*, Aquatic Ecosystem Restoration Foundation, Wisconsin, USA, 3rd edition, 2014.

[21] H. H. Strain and W. A. Svec, "Extraction, separation, estimation, and isolation of the chlorophylls," in *The Chlorophylls*, L. P. Vernon and G. R. Seely, Eds., pp. 21–66, Academic Press, New York, NY, USA, 1966.

[22] M. E. Barbinta-Patrascu, N. Badea, L. G. Țugulea, M. Giurginca, and A. Meghea, "Oxidative stress simulation on artificial membranes- chemiluminescent studies," *Revista de Chimie*, vol. 59, no. 8, pp. 834–837, 2008.

[23] M. E. Barbinta Patrascu, L. Tugulea, and A. Meghea, "Procaine effects on model membranes with chlorophyll*a*," *Revista de Chimie*, vol. 60, no. 4, pp. 337–341, 2009.

[24] S. M. Milenkovic, M. E. Bărbînță-Pătraşcu, G. Baranga, D. Z. Markovic, and L. Țugulea, "Comparative spectroscopic studies on liposomes containing chlorophyll a and chlorophyllide a," *General Physiology and Biophysics*, vol. 32, no. 4, pp. 559–567, 2013.

[25] I. Lacatusu, N. Badea, R. Stan, and A. Meghea, "Novel bio-active lipid nanocarriers for the stabilization and sustained release of sitosterol," *Nanotechnology*, vol. 23, no. 45, Article ID 455702, 2012.

[26] NCCLS M7-A6, "Methods for Dilution Antimicrobial Susceptibility. Test for Bacteria that Grow Aerobically," in *Test for Bacteria that Grow Aerobically*, 6th edition, 2003.

[27] W. B. Hugo and A. D. Russel, *Pharmaceutical Microbiology*, Blackwell science, London, UK, 6th edition, 1998.

[28] M. A. Pfaller, D. J. Sheehan, and J. H. Rex, "Determination of Fungicidal Activities against Yeasts and Molds: Lessons Learned

from Bactericidal Testing and the Need for Standardization," *Clinical Microbiology Reviews*, vol. 17, no. 2, pp. 268–280, 2004.

[29] L. Esteban-Tejeda, K. Zheng, C. Prado et al., "Bone tissue scaffolds based on antimicrobial SiO2-Na2O-Al2O3-CaO-B2O3 glass," *Journal of Non-Crystalline Solids*, vol. 432, pp. 73–80, 2016.

[30] CLSI, *Methods for Determining Bactericidal Activity of Antimicrobial Agents. Approved Guideline, CLSI document M26-A*, Clinical and Laboratory Standards Institute, Pennsylvania, USA, 1998.

[31] C. J. Clancy, H. Huang, S. Cheng, H. Derendorf, and M. H. Nguyen, "Characterizing the effects of caspofungin on Candida albicans, Candida parapsilosis, and Candida glabrata isolates by simultaneous time-kill and postantifungal-effect experiments," *Antimicrobial Agents and Chemotherapy*, vol. 50, no. 7, pp. 2569–2572, 2006.

[32] M. E. Klepser, E. J. Ernst, R. E. Lewis, M. E. Ernst, and M. A. Pfaller, "Influence of test conditions on antifungal time-kill curve results: Proposal for standardized methods," *Antimicrobial Agents and Chemotherapy*, vol. 42, no. 5, pp. 1207–1212, 1998.

[33] M. Balouiri, M. Sadiki, and S. K. Ibnsouda, "Methods for *in vitro* evaluating antimicrobial activity: a review," *Journal of Pharmaceutical Analysis*, vol. 6, no. 2, pp. 71–79, 2016.

[34] CLSI, "Methods for Antimicrobial Dilution and Disk Susceptibility of Infrequently Isolated or Fastidious Bacteria, Approved Guideline, CLSI document M45-A2," 2nd., Ed., Clinical and Laboratory Standards Institute, Pennsylvania, USA, 2010.

[35] W. Raut Rajesh, R. Lakkakula Jaya, S. Kolekar Niranjan, D. Mendhulkar Vijay, and B. Kashid Sahebrao, "Phytosynthesis of silver nanoparticle using *Gliricidia sepium* (Jacq.)," *Current Nanoscience*, vol. 5, no. 1, pp. 117–122, 2009.

[36] J. Ord, H. J. Butler, M. R. McAinsh, and F. L. Martin, "Spectrochemical analysis of sycamore (*Acer pseudoplatanus*) leaves for environmental health monitoring," *Analyst*, vol. 141, no. 10, pp. 1–8, 2016.

[37] S. Kaviya, J. Santhanalakshmi, B. Viswanathan, J. Muthumary, and K. Srinivasan, "Biosynthesis of silver nanoparticles using *Citrus sinensis* peel extract and its antibacterial activity," *Spectrochimica Acta—Part A: Molecular and Biomolecular Spectroscopy*, vol. 79, no. 3, pp. 594–598, 2011.

[38] M. Torab-Mostaedi, "Biosorption of lanthanum and cerium from aqueous solutions using tangerine (*Citrus reticulata*) peel: equilibrium, kinetic and thermodynamic studies," *Chemical Industry and Chemical Engineering Quarterly*, vol. 19, no. 1, pp. 79–88, 2013.

[39] K. R. Namasivayam, R. S. A. Bharani, and M. R. Ansari, "Natural Occurrence of Potential Fungal Biopesticide Nomuraea Rileyi (Farlow) Samson Associated with Agriculture Fields of Tamil Nadu, India and its Compatibility with Metallic Nanoparticles," *Journal of Biofertilizers Biopesticides*, vol. 4, no. 1, pp. 132–139, 2013.

[40] P. R. Mishra, L. A. Shaal, R. H. Müller, and C. M. Keck, "Production and characterization of Hesperetin nanosuspensions for dermal delivery," *International Journal of Pharmaceutics*, vol. 371, no. 1-2, pp. 182–189, 2009.

[41] X. Yang, A. P. Gondikas, S. M. Marinakos et al., "Mechanism of silver nanoparticle toxicity is dependent on dissolved silver and surface coating in *Caenorhabditis elegans*," *Environmental Science & Technology*, vol. 46, no. 2, pp. 1119–1127, 2012.

[42] A. M. Rincón, A. M. Vásquez, and F. C. Padilla, "Chemical composition and bioactive compounds of flour of orange

(*Citrus sinensis*), tangerine (*Citrus reticulata*) and grapefruit (*Citrus paradisi*) peels cultivated in Venezuela," *Archivos Latinoamericanos de Nutrición*, vol. 55, no. 3, pp. 305–310, 2005.

[43] P. N. Navya and H. K. Daima, "Rational engineering of physicochemical properties of nanomaterials for biomedical applications with nanotoxicological perspectives," *Nano Convergenc*, vol. 3, no. 1, pp. 1–14, 2016.

[44] V. Edel-Hermann, M. Sautour, N. Gautheron et al., "A clonal lineage of Fusarium oxysporum circulates in the tap water of different French hospitals," *Applied and Environmental Microbiology*, vol. 82, no. 21, pp. 6483–6489, 2016.

[45] A. G. Varon, S. A. Nouér, G. Barreiros, B. M. Trope, T. Akiti, and M. Nucci, "Antimold prophylaxis may reduce the risk of invasive fusariosis in hematologic patients with superficial skin lesions with positive culture for Fusarium," *Antimicrobial Agents and Chemotherapy*, vol. 60, no. 12, pp. 7290–7294, 2016.

[46] A. D. van Diepeningen, P. Feng, S. Ahmed, M. Sudhadham, S. Bunyaratavej, and G. S. de Hoog, "Spectrum of Fusarium infections in tropical dermatology evidenced by multilocus sequencing typing diagnostics," *Mycoses*, vol. 58, no. 1, pp. 48–57, 2015.

[47] S. Rasti, M. A. Assadi, L. Iranshahi, M. Saffari, H. R. Gilasi, and M. Pourbabaee, "Assessment of microbial contamination and physicochemical condition of public swimming pools in Kashan, Iran," *Jundishapur Journal of Microbiology*, vol. 5, no. 3, pp. 450–455, 2012.

[48] P. Godoy, F. Nunes, V. Silva, J. Tomimori-Yamashita, L. Zaror, and O. Fischman, "Onychomycosis caused by Fusarium solani and Fusarium oxysporum in São Paulo, Brazil," *Mycopathologia*, vol. 157, no. 3, pp. 287–290, 2004.

[49] M. Nucci and E. Anaissie, "Fusarium infections in immunocompromised patients," *Clinical Microbiology Reviews*, vol. 20, no. 4, pp. 695–704, 2007.

[50] C. Krishnaraj, R. Ramachandran, K. Mohan, and P. T. Kalaichelvan, "Optimization for rapid synthesis of silver nanoparticles and its effect on phytopathogenic fungi," *Spectrochimica Acta—Part A: Molecular and Biomolecular Spectroscopy*, vol. 93, pp. 95–99, 2012.

[51] H. S. Sultana, M. Ali, and B. P. Panda, "Influence of volatile constituents of fruit peels of Citrus reticulata Blanco on clinically isolated pathogenic microorganisms under In-vitro," *Asian Pacific Journal of Tropical Biomedicine*, vol. 2, no. 3, pp. S1299–S1302, 2012.

[52] P. Singh, R. Shukla, B. Prakash et al., "Chemical profile, antifungal, antiaflatoxigenic and antioxidant activity of *Citrus maxima* Burm. and *Citrus sinensis* (L.) Osbeck essential oils and their cyclic monoterpene, DL-limonene," *Food and Chemical Toxicology*, vol. 48, no. 6, pp. 1734–1740, 2010.

[53] M. Chutia, P. Deka Bhuyan, M. G. Pathak, T. C. Sarma, and P. Boruah, "Antifungal activity and chemical composition of Citrus reticulata Blanco essential oil against phytopathogens from North East India," *LWT - Food Science and Technology*, vol. 42, no. 3, pp. 777–780, 2009.

[54] W. F. Falco, A. M. Queiroz, J. Fernandes et al., "Interaction between chlorophyll and silver nanoparticles: A close analysis of chlorophyll fluorescence quenching," *Journal of Photochemistry and Photobiology A: Chemistry*, vol. 299, pp. 203–209, 2014.

[55] A. M. Queiroz, A. V. Mezacasa, D. E. Graciano et al., "Quenching of chlorophyll fluorescence induced by silver nanoparticles," *Spectrochimica Acta - Part A: Molecular and Biomolecular Spectroscopy*, vol. 168, pp. 73–77, 2016.

[56] M. I. Hussain and M. J. Reigosa, "A chlorophyll fluorescence analysis of photosynthetic efficiency, quantum yield and photon energy dissipation in PSII antennae of Lactuca sativa L. leaves exposed to cinnamic acid," *Plant Physiology and Biochemistry*, vol. 49, no. 11, pp. 1290–1298, 2011.

[57] A.-J. Miao, K. A. Schwehr, C. Xu et al., "The algal toxicity of silver engineered nanoparticles and detoxification by exopolymeric substances," *Environmental Pollution*, vol. 157, no. 11, pp. 3034–3041, 2009.

[58] A. Barbasz, B. Kreczmer, and M. Oćwieja, "Effects of exposure of callus cells of two wheat varieties to silver nanoparticles and silver salt (AgNO3)," *Acta Physiologiae Plantarum*, vol. 38, no. 3, article no. 76, pp. 1–11, 2016.